TECHNICAL RESEARCH REPORT

SYSTEMS RESEARCH CENTER

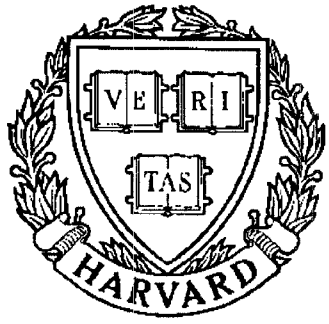

Supported by the National Science Foundation Engineering Research Center Program (NSFD CD 8803012), the University of Maryland, Harvard University, and Industry

Research support for this report has been provided by NASA/Ames grant NCC-2374 and the NSF grant NCR-8814407

Estimation of Multiple Sinusoidal Frequencies Using Truncated Least-Squares Methods

by S.F. Hsieh, K.J.R. Liu and K. Yao

TR 91-68

Estimation of Multiple Sinusoidal Frequencies Using Truncated Least-Squares Methods * †

S.F. Hsieh
Dept. of Communication Engineering
Nat'l Chiao Tung University
Hsinchu, Taiwan 30039

K.J.R. Liu
Electrical Engineering Dept.
Systems Research Center
University of Maryland
College Park, MD 20742

K. Yao
Electrical Engineering Dept.
UCLA
Los Angeles, CA 90024-1594

ABSTRACT

Tufts and Kumaresan (1982) first proposed using a SVD-based method to solve the forward-backward linear prediction (FBLP) least-squares problem for resolving closely spaced frequencies of multiple sinusoids from limited amount of data samples. By imposing an excessive order in the FBLP model and then truncating small singular values to zero, this truncated SVD (TSVD) method yields a low SNR threshold and greatly suppresses spurious frequencies. However, the massive computation required by SVD makes it unsuitable for *real time* super-resolution applications. We propose to use truncated QR methods which are amenable to VLSI implementations, such as systolic arrays, with slightly degraded performances as compared to the TSVD method. Three truncated QR methods for sinusoidal frequency estimation will be considered: (1) truncated QR without column pivoting (TQR); (2) truncated QR with re-ordered columns (TQRR); and (3) truncated QR with column pivoting (TQRP). It is demonstrated that the benefit of the TSVD method for high frequency resolution is achievable under the truncated QR methods with much lower computational cost. Other attractive features of the proposed methods include the ease of updating, which is difficult for the SVD method, and numerical stability. Thus, the TQR methods offer efficient ways for identifying sinusoids closedly clustered in frequencies under stationary and nonstationary conditions. Some results based on the truncated normal equation approach as well as on sufficient conditions for perfect truncations based on truncated QR and SVD methods are considered. Based on the FBLP model, computer simulations and comparisons are provided for different truncation methods under various SNR's. Comparisons of asymptotic performance with large data samples are also given.

*This work is partially supported by the NASA/Ames grant NCC-2374 and the NSF grant NCR-8814407.

†An earlier version of this paper was presented at the *2nd Intern. Workshop on SVD and Signal Processing* and published in the workshop proceedings *SVD and Signal Processing II*, Elsevier Science Publishers, R.J. Vaccaro, ed., 1991.

1 Introduction

In recent years, there is much interest in seeking efficient and effective algorithms for resolving closely spaced sinusoids in the frequency domain as well as in the spatial domain [1, 2, 3, 4, 5, 6, 7, 8, 9]. Generally, a "good" algorithm for spectral estimation should comprise of several factors, i.e., high frequency resolution capability, computational efficiency, updating and downdating capability, and implementable parallel processing structure so that fast real-time applications are possible. Different methods may perform well in some aspects but suffer in the others. While the SVD-based method is well known for its robustness in resolving closely clustered sinusoids, it is not attractive from the other desirable feature points of view. In this paper, we consider several other promising approaches based on the truncated QR and least-squares techniques.

In the pioneering paper of Tufts and Kumaresan [2], a SVD-based method for solving the forward-backward linear prediction(FBLP) least-squares(LS) problem was used to resolve the frequencies of closely spaced sinusoids from limited amount of data samples. By imposing an excessive order in the FBLP model and then truncating small singular values to zero, this truncated SVD method yields a low SNR threshold and greatly suppresses spurious frequencies. However, the massive computations required by SVD makes it unsuitable for *real time* super-resolution applications. We propose to use truncated QR and LS methods which are more amenable to VLSI implementations, such as on systolic arrays[10], with insignificantly degraded performances as compared to the TSVD method. Three different truncated QR methods will be considered, depending on the ordering of the columns of the data matrix. The first one is the truncated QR method without column shuffling (TQR). This method does not change the structure of the data matrix. A QR

decomposition (QRD) of the data matrix is followed by the truncation of the lower right rank-weakly submatrix of the upper-triangular matrix. The second one is the truncated QR method with reordered columns (TQRR). The reordering of the columns is determined in an *a priori* manner [6]. Here truncation is performed on the QRD of the column-reordered data matrix. The computational cost of this TQRR method is the same as that of the first method, except for the column reshuffling. The last one is called truncated QR with column pivoting (TQRP) [11]. This method entails a series of *dynamic* swapping of columns while performing QRD. An additional computational cost is required to monitor the norms of the remaining columns in the dimension-shrinking submatrix such that the first column is replaced by the one with the largest norm in the remaining submatrix. The processing overhead of successive column swapping may be nontrivial and prohibitive in implementing a VLSI structure. All these three truncated QR methods only involve a finite number of computations, while for the TSVD method, the number of iterations required cannot be specified in an exact manner. Based upon MATLAB computations, SVD requires about 5 to 6 times the number of flops as compared to QRD for a dense 50×50 matrix. Furthermore, we should note that QRD only requires a small number of flops for updating when new data are successively appended, while updating SVD is generally much more intractable [12]. A truncated normal equation approach will be shown to be equivalent to the TQR method except for the increased roundoff errors under finite precision computations.

A FBLP model for estimating sinusoidal frequencies is formulated first, followed by an introduction of different truncation methods and the minimum-norm solutions. Finally, comparisons of these three QR and the LS methods to the TSVD method are given based on computer simulations.

2 FBLP Model

Consider a complex-valued data sequence of length n,

$$\tilde{x}_i = \sum_{k=1}^{p} c_k e^{j2\pi f_k i} + w_i \equiv x_i + w_i, \quad i = 1, 2, \cdots, n, \tag{1}$$

where p is the number of sinusoids , complex-valued c_k comprises the amplitudes and phases of each sinusoid, and w_i is an additive white Gaussian noise. We define the signal-to-noise ratio (SNR) as

$$\text{SNR (dB)} = 20\log(\|x\|_2 / \|w\|_2). \tag{2}$$

It can be shown [2] that under noise-free conditions, the frequency locations can be obtained by finding the roots of

$$S(z) = 1 - \sum_{k=1}^{\ell} g_k z^{-k} = 0\,, \tag{3}$$

on the unit circle, where the complex-valued coefficients $g_k's$, $k = 1, 2, \cdots, \ell$, satisfy the following system of FBLP equations

$$\begin{bmatrix} x_\ell & x_{\ell-1} & \cdots & x_1 \\ x_{\ell+1} & x_\ell & \cdots & x_2 \\ \vdots & \vdots & \ddots & \vdots \\ x_{n-1} & x_{n-2} & \cdots & x_{n-\ell} \\ x_2^* & x_3^* & \cdots & x_{\ell+1}^* \\ x_3^* & x_4^* & \cdots & x_{\ell+2}^* \\ \vdots & \vdots & \ddots & \vdots \\ x_{n-\ell+1}^* & x_{n-\ell+2}^* & \cdots & x_n^* \end{bmatrix} \begin{bmatrix} g_1 \\ g_2 \\ \vdots \\ g_\ell \end{bmatrix} = \begin{bmatrix} x_{\ell+1} \\ x_{\ell+2} \\ \vdots \\ x_n \\ x_1^* \\ x_2^* \\ \vdots \\ x_{n-\ell}^* \end{bmatrix} \tag{4}$$

with $\ell \geq p$ representing the order of the prediction model, and $*$ the complex conjugate. We will assume that $2(n-\ell) > \ell$. For simplicity, denote (4) as

$$Ag = b\,, \tag{5}$$

where the data matrix A and the right-hand-side vector b are constructed from the data sequence $\{x_i \mid i = 1,\ldots,n\}$ in a FBLP manner. Symbolically, this will be denoted by $[A \vdots b] \equiv \{x_i \mid i = 1,\ldots,n\}_{\text{FBLP}}$. It is noted that the top half of A represents the forward prediction and is of Toeplitz form while the bottom half represents the backward prediction and is known as a Hankel form. The rank of A is p if $\min\{2(n-\ell),\ell\} \geq p$. When the noise is present, we use an $\tilde{}$ on A and b, i.e., $\tilde{A} = A+E$ and $\tilde{b} = b+e$, to denote the noise-corrupted FBLP model with the additive noise given by $[E \vdots e] \equiv \{w_i \mid i = 1,\ldots,n\}_{\text{FBLP}}$. (5) now becomes the FBLP LS problem of

$$\tilde{A}g \cong \tilde{b}\,, \tag{6}$$

where $\tilde{A}$ usually has full rank due to the perturbation of the noise. One standard approach [2] is to use the TSVD method on (6) to obtain a rank-p approximation of the FBLP matrix $\tilde{A}$, denoted by $\tilde{A}^{(p)}_{SVD}$, followed by solving for a minimum norm LS solution of g given by

$$\tilde{A}^{(p)}_{SVD}\, g \;\cong \tilde{b}\,. \tag{7}$$

Then the frequencies can be computed by finding the phases of the roots of (3) close to the unit circle or searching for the peaks on the pseudo-spectrum $1/|S(exp(j2\pi f)|^2$, $-0.5 \leq f \leq 0.5$. Notice that the proper choice of the prediction order ℓ depends on p, the number of sinusoids, which may or may not be known in advance. Fig. 1 depicts a flowchart diagram summarizing the estimation of harmonics frequencies based on the FBLP model.

3 Truncation Methods

In this section, we consider the rank-p approximation of the FBLP matrix $\tilde{A}$ and subsequently solve for the minimum-norm solution $\tilde{g}^{(p)}$. For many LS problems, ill-conditioning can be troublesome, and truncation methods are known to be useful in stablizing the solutions at the cost of slightly increased residual errors. The rationale is that the condition number[11] of a matrix, defined as the ratio of the largest to the smallest singular values, can be used to characterize a worst case bound on the LS solution when the underlying matrix is subject to some unknown perturbation or round-off errors. When the smaller singular values are discarded, their ill effects on the LS solution are reduced(i.e., stabilized), or we may say that the new condition number of the truncated system is decreased(i.e., stabilized). However, this truncated LS solution, although stablized, will be different from the one that gives the minimum residual; instead, its associated residual with respect to the original *un*truncated linear system will be larger. Therefore, the tradeoff for the truncated linear system lies between an increased stability versus a decreased residual.

Let

$$\tilde{A} = \tilde{U}\tilde{\Sigma}\tilde{V}^H = [\tilde{U}_1\ \tilde{U}_2] \begin{bmatrix} \tilde{\Sigma}_1 & 0 \\ 0 & \tilde{\Sigma}_2 \end{bmatrix} \begin{bmatrix} \tilde{V}_1^H \\ \tilde{V}_2^H \end{bmatrix} \tag{8}$$

and

$$\tilde{A}\Pi = \tilde{Q}\tilde{R} = [\tilde{Q}_1\ \tilde{Q}_2] \begin{bmatrix} \tilde{R}_{11} & \tilde{R}_{12} \\ 0 & \tilde{R}_{22} \end{bmatrix} \tag{9}$$

be the SVD and QRD of the $2(n-\ell) \times \ell$ complex-valued matrix $\tilde{A}$ respectively, where ^{H} denotes the Hermitian of a complex-valued matrix or vector and Π is a column-permutation matrix and will be explained later. $\tilde{\Sigma}_1 = diag(\tilde{\sigma}_1, \ldots, \tilde{\sigma}_p)$ and $\tilde{\Sigma}_2 = diag(\tilde{\sigma}_{p+1}, \ldots, \tilde{\sigma}_\ell)$ represent nonincreasing singular values. $\tilde{R}_{11} \in \mathcal{C}^{p \times p}$, $\tilde{R}_{12} \in \mathcal{C}^{p \times (\ell-p)}$, and $\tilde{R}_{22} \in \mathcal{C}^{\ell-p \times (\ell-p)}$,

while $\tilde{R}$ is an upper-triangular matrix.

$$\tilde{U} = [\tilde{U}_1 \ \tilde{U}_2] = [\tilde{u}_1, \ldots, \tilde{u}_p, \ \tilde{u}_{p+1}, \ldots, \tilde{u}_\ell] \in C^{2(n-\ell)\times \ell}, \tag{10}$$

$$\tilde{V} = [\tilde{V}_1 \ \tilde{V}_2] = [\tilde{v}_1, \ldots, \tilde{v}_p, \ \tilde{v}_{p+1}, \ldots, \tilde{v}_\ell] \in C^{\ell\times \ell}, \tag{11}$$

and

$$\tilde{Q} = [\tilde{Q}_1 \ \tilde{Q}_2] = [\tilde{q}_1, \ldots, \tilde{q}_p, \ \tilde{q}_{p+1}, \ldots, \tilde{q}_\ell] \in C^{2(n-\ell)\times \ell} \tag{12}$$

all have orthonormal columns, i.e., $\tilde{u}_i^H \tilde{u}_j = \tilde{v}_i^H \tilde{v}_j = \tilde{q}_i^H \tilde{q}_j = \delta_{ij}$.

In the absence of noise, $\tilde{\Sigma}_2 = \tilde{R}_{22} = 0$. Here the permutation matrix $\Pi = [\pi_1, \ldots, \pi_\ell]$ is used to represent different methods of performing QRD with column interchanges. Now we want to preserve as much of the energy as possible (with respect to the Frobenius norm defined below) in the trapezoidal matrix $[\tilde{R}_{11} \ \tilde{R}_{12}]$ of (9). Equivalently, we want to leave as little as possible the energy residing in the lower right submatrix $\tilde{R}_{22}$, which will be truncated. This approach amounts to selecting the columns of $\tilde{A}$ in an order such that the column with the largest linear independency will be selected first. This procedure is repeated for the shrinking submatrix.

There are at least 3 possible methods for determining the permutation matrix Π while performing QRD, which are:

1. For QRD with no pivoting, Π is simply an identity matrix.

2. QRD with pre-ordered columns [6] determines Π according to a column index maximum-difference bisection rule. Here we select the first and the ℓ^{th} columns, followed by the column $\lceil \frac{1+\ell}{2} \rceil$ halfway between 1 and ℓ. Then we pick the columns that lie in the mid-way of those ones which are already selected, i.e., $\lceil (1 + \lceil \frac{1+\ell}{2} \rceil)/2 \rceil$, $\lceil (\lceil \frac{1+\ell}{2} \rceil)/2 \rceil + \ell)/2 \rceil$,

and so on. This selection rule does not depend on the real-time data in $\tilde{A}$. The underlying reason for this *ad hoc* fixed-ordering scheme is to provide the selected columns with a possibly maximum differences or minimum linear dependency among these columns. This scheme was motivated due to the nature of the matrix $\tilde{A}$ arranged in the form of (4) consisting of perturbed sums of harmonic sinusoids. As an example, suppose there are 5 columns, then the pre-ordering strategy leads to $[1, 5, 3, 2, 4]$. Thus we have $\Pi = [e_1, e_5, e_3, e_2, e_4]$, where e_i is a dimension ℓ column vector with all zero components except for an one at the i^{th} position.

3. As for QRD with column pivoting [11, p. 233], Π is determined during the QRD process, where $\pi_1 = e_{d_1}$ and $d_1 \in [1, \ell]$ is the index such that $\tilde{a}_{d_1}$ has the largest norm. Continuing with this column-pivoting process on the lower right submatrix yet to be triangularized, we can determine the permutation matrix Π which yields an optimum QRD column ordering strategy in the sense of preserving most energy in the upper trapezoidal submatrix. However, this Π is data-dependent and the extra cost for this pivoting may make it less desirable for some applications.

After forcing those rank-weakly quantities to be zero and preserving the most significant p-rank, we can obtain a rank-p approximate of $\tilde{A}$. These rank-weakly quantities are those entries in the factorized matrix that contribute least significantly to the matrix, or possess the smallest portion of the energy (square of Frobenius norm) of the associated matrix. For TSVD, $\tilde{\Sigma}_2$ is discarded and

$$\tilde{A}^{(p)}_{TSVD} = \tilde{U}_1 \tilde{\Sigma}_1 \tilde{V}_1^H . \tag{13}$$

Similarly, for TQR, the lower-right submatrix $\tilde{R}_{22}$ is discarded and

$$\tilde{A}^{(p)}_{TQR}\,\Pi = \tilde{Q}_1[\tilde{R}_{11}\ \tilde{R}_{12}]. \tag{14}$$

To account for the effect due to truncation, we define the *fractional truncated F-norm* as

$$\mathcal{F}^{(p)} = 1 - \|\tilde{A}^{(p)}\|_F \,/\, \|\tilde{A}\|_F, \tag{15}$$

where $\|\cdot\|_F$ is the Frobenius norm given by

$$\|A\|_F = \sqrt{\sum_i \sum_j |a_{i,j}|^2} = \sqrt{\text{trace }(A^H A)}. \tag{16}$$

Thus we have

$$\mathcal{F}^{(p)}_{TSVD} = \sqrt{\Sigma_{j=p+1}^{\ell}\tilde{\sigma}_j^2 \,/\, \Sigma_{j=1}^{\ell}\tilde{\sigma}_j^2} \tag{17}$$

and

$$\mathcal{F}^{(p)}_{TQR} = 1 - \left(\frac{\|\tilde{R}_{11}\|_F^2 + \|\tilde{R}_{12}\|_F^2}{\|\tilde{R}_{11}\|_F^2 + \|\tilde{R}_{12}\|_F^2 + \|\tilde{R}_{22}\|_F^2}\right)^{1/2}. \tag{18}$$

While

$$0 \le \mathcal{F}^{(p)}_{TSVD} \le \mathcal{F}^{(p)}_{TQRP} \le 1 \tag{19}$$

is valid analytically[11], from extensive computations we also observed the relationships among truncated QR methods to satisfy

$$\mathcal{F}^{(p)}_{TQRP} \le \mathcal{F}^{(p)}_{TQRR} \le \mathcal{F}^{(p)}_{TQR} \le 1. \tag{20}$$

Therefore from the point of view of preserving the Frobenius norm(square root of energy) of a matrix, SVD provides the optimum truncation, with TQRP being next, while TQR and TQRR truncate even more.

4 Perturbation of Matrix Decomposition and Perfect Truncation

In this section, we examine the effects of the noise matrix E on the decompositions of $\tilde{A} = A + E$, and associated sufficient conditions for perfect truncations based on truncated QR and SVD methods. For simplicity, we only consider the QRD method without pivoting. Since the noise-free data matrix A has rank p, we have

$$A = [Q_1 \vdots Q_2] \begin{bmatrix} R_{11} & R_{12} \\ 0 & 0 \end{bmatrix} \tag{21}$$

$$= [Q_1 R_{11} \vdots Q_1 R_{12}] . \tag{22}$$

The noise-perturbed data matrix $\tilde{A}$ can be written as

$$\tilde{A} = A + E \tag{23}$$

$$= [Q_1 \vdots Q_2] \begin{bmatrix} R_{11} & R_{12} \\ 0 & 0 \end{bmatrix} + [Q_1 \vdots Q_2] \begin{bmatrix} E_{11}^* & E_{12}^* \\ E_{21}^* & E_{22}^* \end{bmatrix} \tag{24}$$

$$= [Q_1 \vdots Q_2] \begin{bmatrix} R_{11} + E_{11}^* & R_{12} + E_{12}^* \\ E_{21}^* & E_{22}^* \end{bmatrix} \tag{25}$$

$$= [Q_1 \vdots Q_2] \begin{bmatrix} Q_{11}^* & Q_{12}^* \\ Q_{21}^* & Q_{22}^* \end{bmatrix} \begin{bmatrix} \tilde{R}_{11} & \tilde{R}_{12} \\ 0 & \tilde{R}_{22} \end{bmatrix} \tag{26}$$

$$= [\tilde{Q}_1 \vdots \tilde{Q}_2] \begin{bmatrix} \tilde{R}_{11} & \tilde{R}_{12} \\ 0 & \tilde{R}_{22} \end{bmatrix}, \tag{27}$$

where

$$\tilde{Q}_1 = Q_1 Q_{11}^* + Q_2 Q_{21}^*, \tag{28}$$

$$\tilde{Q}_2 = Q_1 Q_{12}^* + Q_2 Q_{22}^*, \tag{29}$$

and

$$\begin{bmatrix} Q_{11}^* & Q_{12}^* \\ Q_{21}^* & Q_{22}^* \end{bmatrix} \begin{bmatrix} \tilde{R}_{11} & \tilde{R}_{12} \\ 0 & \tilde{R}_{22} \end{bmatrix} = \text{QRD} \left\{ \begin{bmatrix} R_{11} + E_{11}^* & R_{12} + E_{12}^* \\ E_{21}^* & E_{22}^* \end{bmatrix} \right\}, \tag{30}$$

with QRD$\{\cdot\}$ denoting the QR decomposition operator on the matrix in $\{\cdot\}$.

After truncation, we have

$$\tilde{A}_{QR}^{(p)} = [\tilde{Q}_1 \vdots \tilde{Q}_2] \begin{bmatrix} \tilde{R}_{11} & \tilde{R}_{12} \\ 0 & 0 \end{bmatrix} \tag{31}$$

$$= [\tilde{Q}_1 \tilde{R}_{11} \vdots \tilde{Q}_1 \tilde{R}_{12}]. \tag{32}$$

Let us define a *perfect truncation* as the case when

$$\tilde{A}_{QR}^{(p)} = A\,. \tag{33}$$

That is, the original noise-free data matrix A can be fully recovered after truncating the rank-weakly part of the factorization of the noise-corrupted matrix $\tilde{A}$. A sufficient condition for (33) (i.e., (32) to be equal to (22)), is for the noise matrix E to satisfy $E_{11}^* = E_{12}^* = E_{21}^* = 0$, where

$$E = [Q_1 \vdots Q_2] \begin{bmatrix} E_{11}^* & E_{12}^* \\ E_{21}^* & E_{22}^* \end{bmatrix} \tag{34}$$

$$= [Q_1 \vdots Q_2] \begin{bmatrix} 0 & 0 \\ 0 & E_{22}^* \end{bmatrix} \tag{35}$$

$$= [0 \vdots Q_2 E_{22}^*]\,. \tag{36}$$

(36) reveals that the first p columns of $\tilde{A}$ are noise-free and the rest of the columns all reside in the orthogonal-complement column space of the data matrix A.

Similarly for SVD, we have

$$\tilde{A} = A + E \tag{37}$$

$$= [U_1 \vdots U_2] \begin{bmatrix} \Sigma_1 & 0 \\ 0 & 0 \end{bmatrix} \begin{bmatrix} V_1^H \\ V_2^H \end{bmatrix} + [U_1 \vdots U_2] \begin{bmatrix} \mathcal{E}_{11}^* & \mathcal{E}_{12}^* \\ \mathcal{E}_{21}^* & \mathcal{E}_{22}^* \end{bmatrix} \begin{bmatrix} V_1^H \\ V_2^H \end{bmatrix} \tag{38}$$

$$= [U_1 \vdots U_2] \begin{bmatrix} \Sigma_1 + \mathcal{E}_{11}^* & \mathcal{E}_{12}^* \\ \mathcal{E}_{21}^* & \mathcal{E}_{22}^* \end{bmatrix} \begin{bmatrix} V_1^H \\ V_2^H \end{bmatrix} \tag{39}$$

$$= [U_1 \vdots U_2] \begin{bmatrix} U_{11}^* & U_{12}^* \\ U_{21}^* & U_{22}^* \end{bmatrix} \begin{bmatrix} \tilde{\Sigma}_1 & 0 \\ 0 & \tilde{\Sigma}_2 \end{bmatrix} \begin{bmatrix} V_{11}^{*H} & V_{21}^{*H} \\ V_{12}^{*H} & V_{22}^{*H} \end{bmatrix} \begin{bmatrix} V_1^H \\ V_2^H \end{bmatrix} \tag{40}$$

$$= [\tilde{U}_1 \vdots \tilde{U}_2] \begin{bmatrix} \tilde{\Sigma}_1 & 0 \\ 0 & \tilde{\Sigma}_2 \end{bmatrix} \begin{bmatrix} \tilde{V}_1^H \\ \tilde{V}_2^H \end{bmatrix}, \tag{41}$$

where

$$[\tilde{U}_1 \vdots \tilde{U}_2] = [U_1 \vdots U_2] \begin{bmatrix} U_{11}^* & U_{12}^* \\ U_{21}^* & U_{22}^* \end{bmatrix}, \tag{42}$$

$$[\tilde{V}_1 \vdots \tilde{V}_2] = [V_1 \vdots V_2] \begin{bmatrix} V_{11}^* & V_{12}^* \\ V_{21}^* & V_{22}^* \end{bmatrix}, \tag{43}$$

and

$$\begin{bmatrix} U_{11}^* & U_{12}^* \\ U_{21}^* & U_{22}^* \end{bmatrix} \begin{bmatrix} \tilde{\Sigma}_1 & 0 \\ 0 & \tilde{\Sigma}_2 \end{bmatrix} \begin{bmatrix} V_{11}^{*H} & V_{21}^{*H} \\ V_{12}^{*H} & V_{22}^{*H} \end{bmatrix} = \text{SVD} \left\{ \begin{bmatrix} \Sigma_1 + \mathcal{E}_{11}^* & \mathcal{E}_{12}^* \\ \mathcal{E}_{21}^* & \mathcal{E}_{22}^* \end{bmatrix} \right\}, \tag{44}$$

with SVD$\{\cdot\}$ denoting the SVD operator on the matrix in $\{\cdot\}$.

We also notice that to achieve perfect truncation for the SVD method, we need

$$\tilde{A}_{SVD}^{(p)} = \tilde{U}_1 \tilde{\Sigma}_1 \tilde{V}_1^H = A \,. \tag{45}$$

A sufficient condition for (45) is $\mathcal{E}_{11}^* = \mathcal{E}_{12}^* = \mathcal{E}_{21}^* = 0$ (i.e., $E = U_2 \mathcal{E}_{22}^* V_2^H$) and the largest singular value of E is less than the smallest singular value of Σ_1, or equivalently, the row and

column spaces of E must be orthogonal to those of A, and there exists a gap between the singular values of A and E such that even the weakest signal subspace will not be corrupted by any erroneous noise space.

5 Minimum-norm Solutions

After truncation, the FBLP LS problem becomes rank-deficient, hence the minimum-norm LS solution is desired in order to suppress those spurious harmonics in the pseudo-spectrum. The following lemma gives the minimum-norm solution for a rank-deficient LS problem.

Lemma: (Minimum-norm solution) For an underdetermined LS problem,

$$B\mathbf{y} = \mathbf{c}, \qquad (B \in \mathcal{C}^{p\times\ell}, \mathbf{c} \in \mathcal{C}^{p}, p \leq \ell), \tag{46}$$

with rank(B)=p. The minimum-norm solution $\hat{\mathbf{y}}$ is in the row space of B.

Proof: Suppose B has full row rank and $\hat{\mathbf{y}}$ belongs to the row space of B, i.e., $\hat{\mathbf{y}} = B^H\mathbf{z}$, then there exists a unique solution $\hat{\mathbf{y}} = B^H\mathbf{z}$ since $\mathbf{z} = (BB^H)^{-1}\mathbf{c}$ is unique. Suppose there are other solutions of the form $\mathbf{y} = \hat{\mathbf{y}} + \mathbf{y}^{\perp}$, where $\mathbf{y}^{\perp}$ lies in the space perpendicular to the row space of B, i.e., $B\mathbf{y}^{\perp} = 0$. Then it is obvious that

$$\|\mathbf{y}\|^2 = \|\hat{\mathbf{y}}\|^2 + \|\mathbf{y}^{\perp}\|^2 \geq \|\hat{\mathbf{y}}\|^2. \tag{47}$$

So

$$\hat{\mathbf{y}} = arg\ \min\{\|\mathbf{y}\| \mid B\mathbf{y} = \mathbf{c}\}.\square$$

For simplicity, let Π be an identity in the QRD case. To avoid the cumbersome normal-equation-like computation of the minimum norm solution, $B^H(BB^H)^{-1}\mathbf{c}$, with $B = [\tilde{R}_{11}\ \tilde{R}_{12}]$ and $\mathbf{c} = \tilde{Q}_1^H\tilde{b}$, we can firstly perform a *backward* QR decomposition on

the conjugate transpose of $[\tilde{R}_{11}\,\tilde{R}_{12}]$ to obtain the same solution as given in the above lemma without fill-in's(the newly introduced nonzero entities while performing QRD). Ill-conditioning will not occur because the diagonal elements are sufficiently large in the trapezoidal truncated matrix. By doing backward modified Gram-Schmidt orthogonalization[11] procedure, we can have

$$B^H = \begin{bmatrix} \tilde{R}_{11}^H \\ \\ \tilde{R}_{12}^H \end{bmatrix} = TL, \qquad (T \in C^{\ell \times p}; L \in C^{p \times p}), \tag{48}$$

with L being lower triangular. Here the columns of $T = [\mathbf{t}_1, \ldots, \mathbf{t}_p]$ (satisfying $T^H T = I$) are computed in a backward manner, i.e, from $\mathbf{t}_p$ to $\mathbf{t}_1$, and the diagonal elements of L are computed from the lower right toward the upper left. We note that the minimum solution for the truncated QR method is given by

$$\begin{aligned} g_{TQR}^p &= B^H(BB^H)^{-1}\mathbf{c} \\ &= TL(L^H T^H T L)^{-1}\mathbf{c} \\ &= T(L^{-H}\mathbf{c}), \end{aligned} \tag{49}$$

where it is also noted that a backward substitution is required in the computation of $L^{-H}\mathbf{c}$.

Therefore the minimum-norm LS solution can be obtained via the following procedure:

1. Do QRD on the augmented matrix $[\tilde{A} \vdots \tilde{b}]$ (with possibly column pivoting);

2. Take the transpose of the trapezoidal upper triangular matrix. Do backward QRD (save the orthogonal matrix T) ;

3. Apply backward substitution on the transpose of lower-triangular matrix obtained in step (2) and the updated right-hand-side in step (1), followed by (49).

According to this lemma, a minimum-norm solution vector $g^{(p)}$ must lie in the row space of the rank-reduced matrix $\tilde{A}^{(p)}$, namely, the row space of $\tilde{V}_1^H$ or $[\tilde{R}_{11}\ \tilde{R}_{12}]$. For TSVD it is given by

$$g_{TSVD}^{(p)} = \tilde{V}_1 \tilde{\Sigma}_1^{-1} \tilde{U}_1^H \tilde{b}, \tag{50}$$

or

$$g_{TSVD}^{(p)} = \sum_{j=1}^{p} \frac{\tilde{u}_j^H \tilde{b}}{\tilde{\sigma}_j} \tilde{v}_j \ . \tag{51}$$

To obtain $g_{TQR}^{(p)}$, we can perform QRD on the right of the trapezoidal upper-triangular matrix in (14) to zero out $\tilde{R}_{12}$ and also obtain the orthonormal row space, $\tilde{T}^H$, of $[\tilde{R}_{11}\ \tilde{R}_{12}]$. That is

$$\tilde{A}_{TQR}^{(p)}\, \Pi = \tilde{Q}_1 [\tilde{R}_{11}\ \tilde{R}_{12}] \ = \tilde{Q}_1 \tilde{L}^H \tilde{T}^H \ , \tag{52}$$

where $\tilde{T} = [\tilde{t}_1, \ldots, \tilde{t}_p] \in \mathcal{C}^{\ell \times p}$ has orthonormal columns and $\tilde{L}^H \in \mathcal{C}^{p \times p}$ is an upper-triangular matrix. This is sometimes called a *complete orthogonal factorization* [11, p. 236], and we can consider it as a two-sided direct unitary transformations on a rank-deficient matrix to compress all the energy of a matrix into a *square upper-triangular* matrix. This resembles the SVD method where two-sided iterative unitary transformations are applied to reduce a matrix into a *diagonal* matrix. Then from (49) and (52) the minimum-norm solution follows by

$$g_{TQR}^{(p)} \ = \ \Pi \begin{bmatrix} \tilde{R}_{11}^H \\ \tilde{R}_{12}^H \end{bmatrix} (\tilde{R}_{11}\tilde{R}_{11}^H + \tilde{R}_{12}\tilde{R}_{12}^H)^{-1} \tilde{Q}_1^H \tilde{b} \tag{53}$$

$$= \ \Pi \tilde{T} \tilde{L}^{-H} \tilde{Q}_1^H \tilde{b} \ . \tag{54}$$

It is noted that if no truncation is performed at all and $\tilde{A}$ has full column rank ℓ, then the LS solution from the FBLP model is either obtained from SVD as

$$\tilde{g} \ = \ \tilde{V}_1 \tilde{\Sigma}_1^{-1} \tilde{U}_1^H \tilde{b} \ + \ \tilde{V}_2 \tilde{\Sigma}_2^{-1} \tilde{U}_2^H \tilde{b}$$

$$= \sum_{j=1}^{p} \frac{\tilde{u}_j^H \tilde{b}}{\tilde{\sigma}_j} \tilde{v}_j + \sum_{j=p+1}^{\ell} \frac{\tilde{u}_j^H \tilde{b}}{\tilde{\sigma}_j} \tilde{v}_j$$

$$= g_{TSVD}^{(p)} + \sum_{j=p+1}^{\ell} \frac{\tilde{u}_j^H \tilde{b}}{\tilde{\sigma}_j} \tilde{v}_j \,, \tag{55}$$

or from QRD as

$$\begin{aligned} \tilde{g} &= \Pi \begin{bmatrix} \tilde{R}_{11} & \tilde{R}_{12} \\ 0 & \tilde{R}_{22} \end{bmatrix}^{-1} \begin{bmatrix} \tilde{Q}_1^H \tilde{b} \\ \tilde{Q}_2^H \tilde{b} \end{bmatrix} \\ &= \Pi \begin{bmatrix} \tilde{R}_{11}^{-1} & -\tilde{R}_{11}^{-1} \tilde{R}_{12} \tilde{R}_{22}^{-1} \\ 0 & \tilde{R}_{22}^{-1} \end{bmatrix} \begin{bmatrix} \tilde{Q}_1^H \tilde{b} \\ \tilde{Q}_2^H \tilde{b} \end{bmatrix} \\ &= \Pi \begin{bmatrix} \tilde{R}_{11}^{-1} \tilde{Q}_1^H \tilde{b} - \tilde{R}_{11}^{-1} \tilde{R}_{12} \tilde{R}_{22}^{-1} \tilde{Q}_2^H \tilde{b} \\ \tilde{R}_{22}^{-1} \tilde{Q}_2^H \tilde{b} \end{bmatrix} \end{aligned} \tag{56}$$

Because $\tilde{\Sigma}_2$ and $\tilde{R}_{22}$ are both nearly zero under a high SNR condition, slight variations on them will cause significant perturbations in the solution vector $\tilde{g}$ and hence leads to many spurious frequencies in the pseudo-spectrum. Now it becomes clear why one truncates these rank-weakly quantities to remedy these ill-conditions from the view point of numerical stability and also prefilters some stray noise in an attempt to guard against possible contaminations in the pseudo-spectrum.

For many problems, the conservative approach of over-modeling (i.e., $\ell >> p$) is preferred [2, 5] to taking $\ell \gtrsim p$, since we can later *truncate* some noises that reside in the null space which is orthogonal to the signal space. The advantage of over-modeling is to provide some extra dimensions to *trap* the stray noises and then remove them by truncation. This is an effective way of enhancing the SNR. However, there is always the danger that some signal has been mistakably truncated in low SNR cases where ambiguous changes in the truncated F-norm is possible. On the other hand, spurious frequencies are still very likely

to occur when there is insufficient truncation of the rank of the data matrix.

6 Truncated Normal Equation Approach

Up to now, the matrix decompositions are performed with the direct data, hence the condition number of the problem is not increased. It is interesting to see that there also exists a truncated normal equation (TNE) solution which computes the minimum norm solution for the covariance data. We show that essentially this TNE method is mathematically equivalent to the TQR method except for increased roundoff errors under finite precision computations.

An *un*truncated least-squares solution for (6) using the normal equation approach is to solve

$$\tilde{A}^H \tilde{A} g = \tilde{A}^H \tilde{b}. \tag{57}$$

If we rewrite $\tilde{A}$ as $[\tilde{A}_1 \vdots \tilde{A}_2] = [\tilde{A}_1 \vdots \tilde{A}_1 \tilde{F} + N]$, where $\tilde{F} \in \mathcal{C}^{p \times (\ell - p)}$ represents the projection of $\tilde{A}_2$ onto $\tilde{A}_1$ and $N \in \mathcal{C}^{2(n-\ell) \times (\ell - p)}$ represents the remaining residual. Therefore, columns of $\tilde{A}_1 \in \mathcal{C}^{2(n-\ell) \times p}$ and $N \in \mathcal{C}^{2(n-\ell) \times (\ell - p)}$ are orthogonal to each other. Under high SNR cases, N is close to a zero matrix, and in the extreme case when the noise is absent, N is equal to zero. Then (57) can be rewritten as

$$\begin{bmatrix} \tilde{A}_1^H \tilde{A}_1 & \tilde{A}_1^H \tilde{A}_2 \\ \tilde{A}_2^H \tilde{A}_1 & \tilde{A}_2^H \tilde{A}_2 \end{bmatrix} g = \begin{bmatrix} \tilde{A}_1^H \tilde{b} \\ \tilde{A}_2^H \tilde{b} \end{bmatrix} \tag{58}$$

or

$$\begin{bmatrix} \tilde{A}_1^H \tilde{A}_1 & \tilde{A}_1^H \tilde{A}_2 \\ \tilde{F}^H \tilde{A}_1^H \tilde{A}_1 + N^H \tilde{A}_1^H & \tilde{F}^H \tilde{A}_1^H \tilde{A}_2 + N^H \tilde{A}_2^H \end{bmatrix} g = \begin{bmatrix} \tilde{A}_1^H \tilde{b} \\ \tilde{A}_2^H \tilde{b} \end{bmatrix}. \tag{59}$$

We can see that as N goes to zero, the bottom $(\ell - p)$ equations in (59) become redundant, because they are merely equal to $\tilde{F}^H$ times the top p equations. Therefore, a truncated

normal equation (TNE) can be defined by discarding the almost-redundant bottom $(\ell - p)$ equations in (59).

Similarly, a minimum norm solution (from the above Lemma) follows by

$$g_{TNE}^{(p)} = \begin{bmatrix} \tilde{A}_1^H \tilde{A}_1 \\ \tilde{A}_2^H \tilde{A}_1 \end{bmatrix} [\tilde{A}_1^H \tilde{A}_1 \tilde{A}_1^H \tilde{A}_1 + \tilde{A}_1^H \tilde{A}_2 \tilde{A}_2^H \tilde{A}_1]^{-1} \cdot (\tilde{A}_1^H \tilde{b}). \tag{60}$$

It remains to show that TQR and TNE methods in eqns. (53) and (60) are mathematically equivalent. To this end, we can replace $\tilde{A}_1$ by $\tilde{Q}_1 \tilde{R}_{11}$ and $\tilde{A}_2$ by $\tilde{Q}_1 \tilde{R}_{12} + \tilde{Q}_2 R_{22}$, hence we have $\tilde{A}_1^H \tilde{A}_1 = \tilde{R}_{11}^H \tilde{R}_{11}$ and $\tilde{A}_2^H \tilde{A}_1 = \tilde{R}_{12}^H \tilde{R}_{11}$. After some manipulations, (60) can be written as

$$g_{TNE}^{(p)} = \begin{bmatrix} \tilde{R}_{11}^H \\ \tilde{R}_{12}^H \end{bmatrix} \tilde{R}_{11}^H [(\tilde{R}_{11} \tilde{R}_{11}^H + \tilde{R}_{12} \tilde{R}_{12}^H) \tilde{R}_{11}]^{-1} \cdot (\tilde{Q}_1^H \tilde{b}) \,, \tag{61}$$

which is equal to $g_{TQR}^{(p)}$ in (53) where Π is an identity.

We must note that although TQR and TNE methods are mathematically equivalent, the former is much favorable under finite precision computation. The rationale is that the TQR method always deals with the direct data, while the TNE method works on the covariance data where the dynamic range of data is inevitably squared. Therefore the TNE method is more susceptible to roundoff errors.

7 Simulation Results

Finally, we present various computer simulations based on the following model. Let $\tilde{x}_i = cos(2\pi f_1 i) + cos(2\pi f_2 i) + w_i, i = 1, 2, \cdots, 48$, with $f_1 = .125, f_2 = .135, \ell = 36$ and $\{w_i\}$ is a white Gaussian random sequence. The frequencies are determined by the phases (from 0 to π) of complex roots closest to the unit circle. For TQRR, we pre-permute the columns of the

FBLP matrix in the order of: {1 36 18 9 27 5 ... } as suggested by [6]. We will consider three quantities on the evaluation of the performances. The first one is the frequency bias, which is defined as the difference of the true and estimated frequencies. The standard deviation of the estimated frequency is our second performance measure. The last one is the distance of the third principal root to the unit circle. Here we represent the principal root as those roots that are close to the unit circle. Ideally we should have only 2 principal roots (due to the two sinusoids if we only consider those roots with phases within $[0, \pi]$), falling exactly on the unit circle, while all the others are inside the unit circle. Under moderate SNR conditions, a third principal root may be mistaken as a third candidate harmonic, if its distance to the unit circle is approximately equal to the first 2 principal roots. An even worse condition may occur when the true harmonic falls behind (i.e., further away from the unit circle) an spurious harmonic due to the random noise. This is similar to the case that a noise subspace enters the signal subspace. Therefore, a good separation of the 3rd harmonic from the unit circle not only decreases the chance of mistaking false harmonics but also increases our confidence on estimating the true number of harmonics.

Two classes of comparisons will be considered in the following curves. The first one is to compare these truncation methods under various SNR from 0 to 50 dB. The second is to observe the asymptotic performance by fixing the order $\ell = 36$, and increasing the number of observed data samples. 100 independent simulations are used to obtain the statistical means and standard deviations.

Fig. 2 gives the average fractional truncated Frobenius norms of (16) versus SNR when we preserve only the four most significant ranks of the FBLP matrix for the five different methods. This confirms their relationships in (19) and (20) and also shows that the trun-

cated energy decreases monotonically as SNR increases. Fig. 3 and 4 show the averages of the frequency biases for the two harmonic frequencies. We define the average frequency bias as $E(\tilde{f}_k) - f_k, \quad k = 1, 2$, where $E(\tilde{f}_k)$ is the ensemble average of $\tilde{f}_k$, which is the estimated frequency for f_k. Fig. 5 and 6 show the standard deviations of $\tilde{f}_1$ and $\tilde{f}_2$. We can see that TQRP competes quite well with TSVD, while TQRR performs slightly worse than TQRP but better than TQR without pivoting. Fig. 7 and 8 show the distances to the unit circle of the first 2 dominant roots that are closest to the unit circle. Fig. 9 gives the distance to the unit circle of the third closest root. Since this third root is a false one, it should be far away from the unit circle to allow for easy determination of number of harmonics.

If we fix the SNR= 10 dB and the order of the FBLP model to be $\ell = 36$, as more data are collected, the ill effect due to noise should be asymptotically smoothed out. Fig. 10 shows the combined average frequency bias (defined as the sum of the absolute values of the biases for f_1 and f_2) verses the number of data samples. Fig. 11 shows the curves of various combined standard deviations of the estimated frequencies which is defined as the square root of the sum of squares of the standard deviations of each frequency estimate. Fig. 12 depicts the mean distances to the unit circle of the false harmonics. From Fig. 10 to 12, it is clear that under moderate SNR conditions, the performances of TQRP closely follow that of TSVD.

8 Conclusions

While a myriad of researches have been focused on SVD and eigen-decomposition analysis of narrowly spaced harmonic frequency estimations [2, 5, 7], very few have been directed towards the QRD approaches. Owing to the iterative massive computations and the diffi-

culty encountered in updating the decompositions [12] when new data are acquired under time-varying conditions, these SVD and eigen-based approaches are ill suited for real time applications. It is well known [11] that QRD is numerically as stable as SVD, requires much less computational cost, easy to update(and/or downdate), and amenable to VLSI implementations. The slightly degraded performance for these truncated QR methods is greatly compensated by all the benefits mentioned above. As well known, the performance of the LS method is usually much worse than those of the QR and SVD methods.

Table 1 summarizes the comparisons among different truncation methods. We conclude that TQR is the simplest and can be performed easily in a real time updating, but may suffer significant degradation. TQRP provides almost the same performance as SVD, but is not easy to implement in real time processing in that the difficult column reshuffling is required while performing QRD with pivoting. TQRR provides a good compromise between the above two and can also be implemented for systolic array processing. The LS method is simple to implement and update but has a poor frequency estimation capability.

References

[1] Ralph Schmidt. "Multiple emitter location and signal parameter estimation". In *Proc. RADC Spectrum Estimation Workshop*, pages 243–258, 1979.

[2] D. W. Tufts and R. Kumaresan. "Estimation of frequencies of multiple sinusoids: making linear prediction perform like maximum likelihood". *Proc. IEEE*, 70(9):975–989, Sept 1982.

[3] Thomas P. Bronez and James A. Cadzow. "An algebraic approach to superresolution

array processing". *IEEE Trans. on Aerospace and Electronic Systems*, AES-19(1):123–133, Jan. 1983.

[4] M. Kaveh and A. J. Barabell. "The statistical performance of MUSIC and the minimum norm algorithms in resolving plane waves in noise". *IEEE Trans. on Acous., Speech, and Signal Processing*, ASSP-34(2):331–340, Apr. 1986.

[5] B. D. Rao. "Perturbation analysis of an SVD-based linear prediction method for estimating the frequencies of multiple sinusoids". *IEEE Trans. Acoust., Speech, Signal Processing*, 36(7):1026–1035, July 1988.

[6] J. P. Reilly, W. G. Chen, and K. M. Wong. "A fast QR-based array-processing algorithm". In *SPIE Vol. 975 Advanced Algo. and Arch. for Signal Proc III*, pages 36–47, 1988.

[7] S. L. Marple Jr. "A tutorial overview of modern spectral estimation". In *IEEE ICASSP*, pages 2152–2157, 1989.

[8] B. D. Rao and K. V. S. Hari. "Statistical performance analysis of the minimum-norm method". In *IEEE ICASSP*, pages 2760–2763, 1989.

[9] D. W. Tufts, R. J. Vaccaro, and A. C. Kot. "Analysis of estimation of signal parameters by linear-prediction at high SNR using matrix approximation". In *IEEE ICASSP*, pages 2194–2197, 1989.

[10] W. M. Gentleman and H. T. Kung. "Matrix triangularization by systolic array". In *Proc. SPIE, vol. 298: Real-time signal processing IV*, pages 19–26, Bellingham, Washington, 1981. Society of Photo-optical Instrumentaion Engineers.

[11] G. H. Golub and C. F. Van Loan. *"Matrix computations"*. Johns Hopkins University Press, Baltimore, MD, 2nd edition, 1989.

[12] J. R. Bunch and C. P. Nielsen. "Updating the singular value decomposition". *Numerische Mathematik*, 31:111–129, 1978.

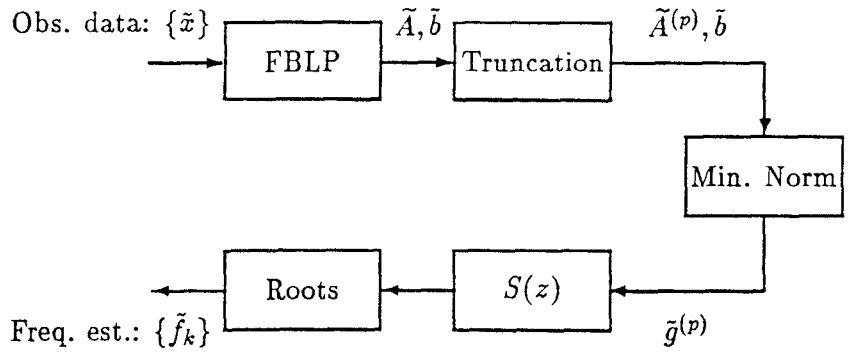

Figure 1: Block diagram for sinusoidal frequency estimation based on the FBLP model.

Table 1: Comparisons of truncated least-squares methods.

	Freq. est.	Comput. cost	VLSI	updating
TSVD	excellent	very high	complex	difficult
TQRP	very good	medium	medium	medium
TQRR	good	fair	fair	easy
TQR	fair	fair	fair	easy
LS	poor	low	low	easy

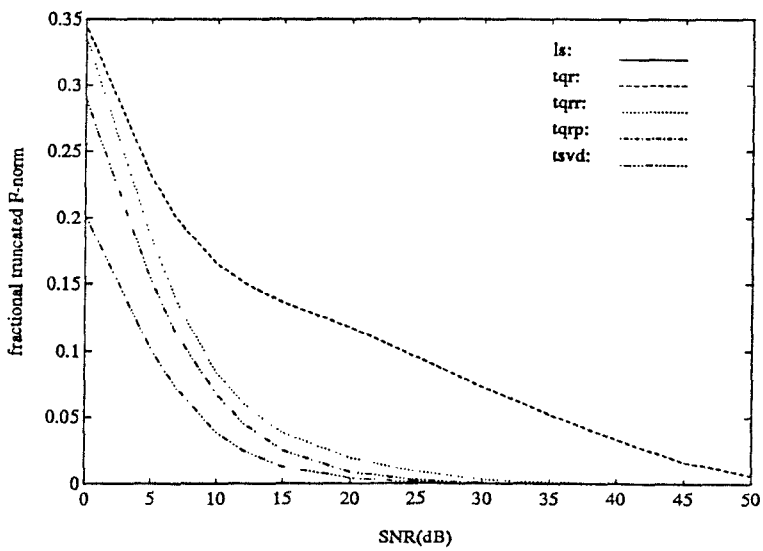

Figure 2: Average fractional truncated Frobenius norms.

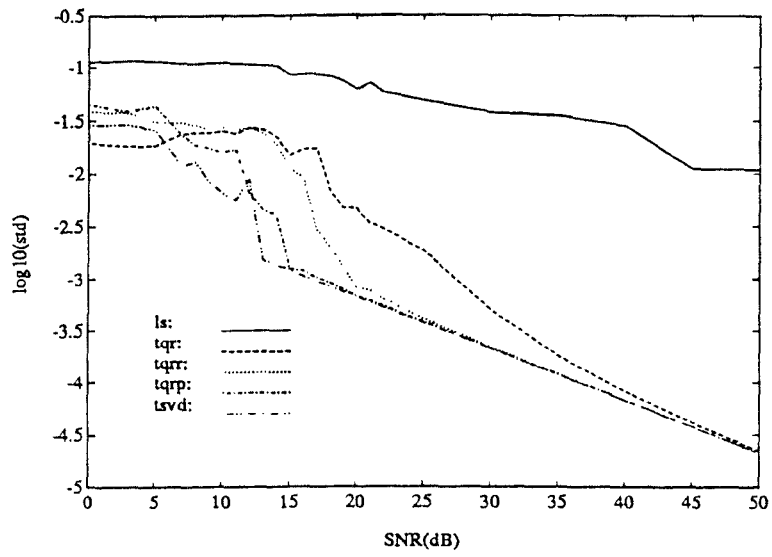

Figure 5: Standard deviations for estimating $f_1 = .125$ using a 24×36 FBLP matrix.

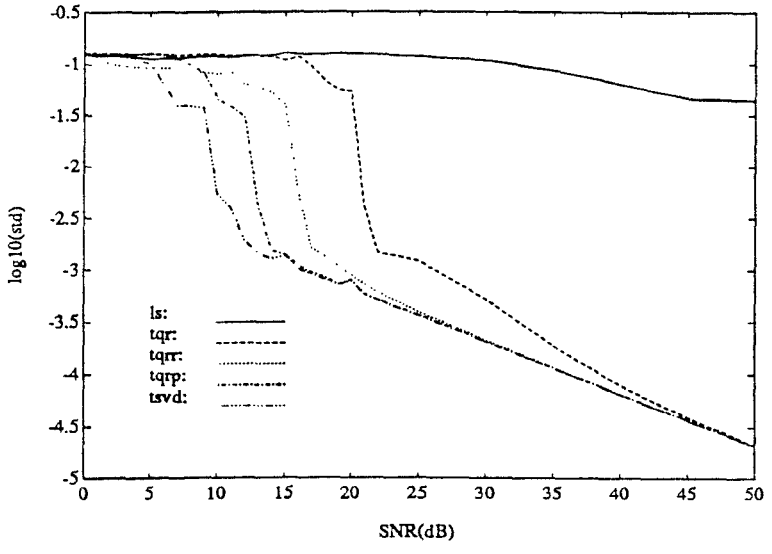

Figure 6: Standard deviations for estimating $f_2 = .135$ using a 24×36 FBLP matrix.

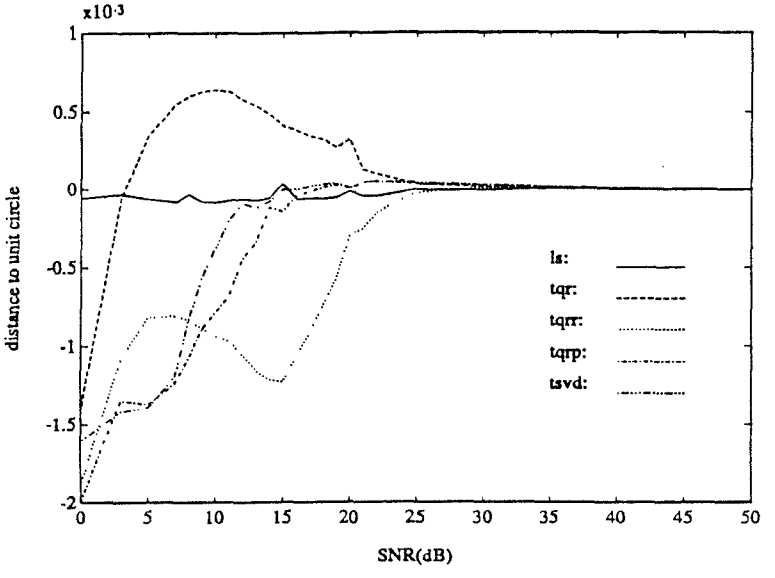

Figure 7: Mean distances to unit circle of the roots of the 1st harmonic freq. estimator vs. SNR.

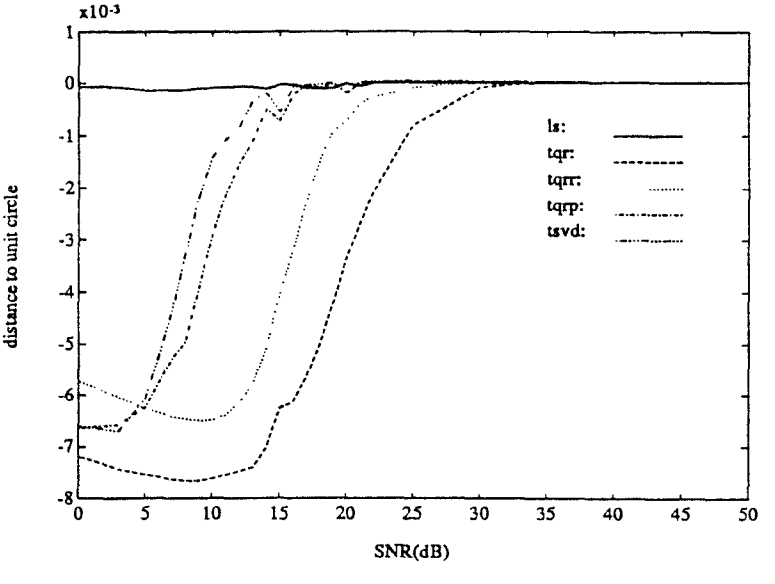

Figure 8: Mean distances to unit circle of the roots of the 2nd harmonic freq. estimator vs. SNR.

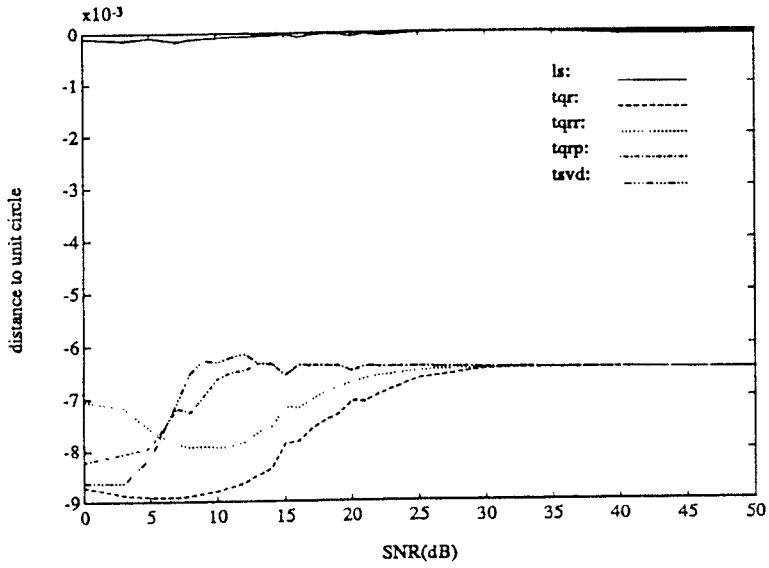

Figure 9: Mean distances to unit circle of the roots of the 3rd (false) harmonic freq. estimator vs. SNR

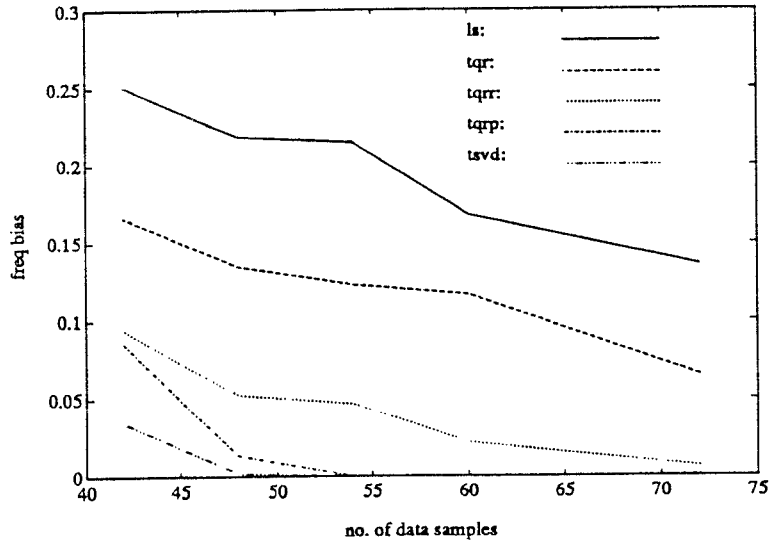

Figure 10: Mean freq bias vs. no. of data samples for $f = \{.125, .135\}$, SNR=10dB, and order=36.

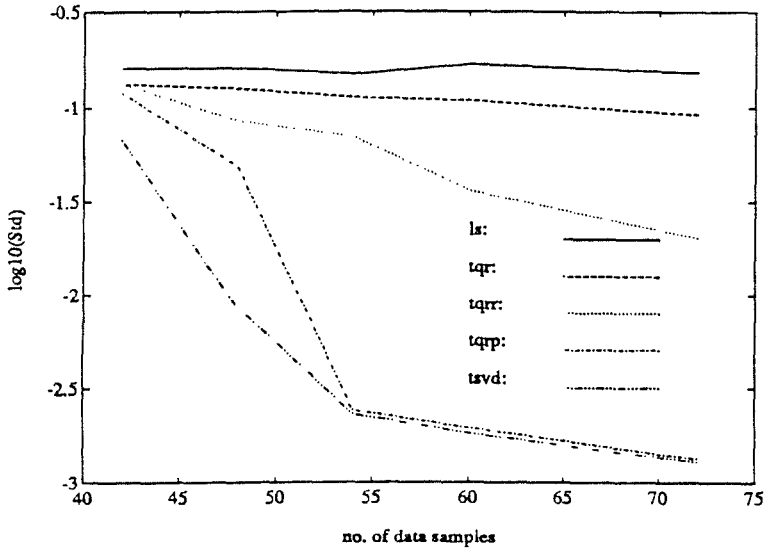

Figure 11: Standard deviations of estimates vs. no. of data samples for $f = \{.125, .135\}$, SNR=10dB, and order=36.

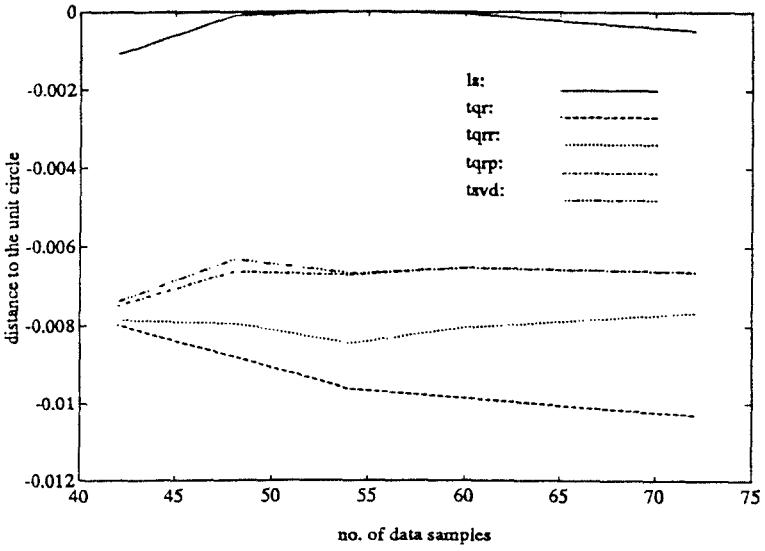

Figure 12: Mean distances to unit circle of the roots of the 3rd (false) harmonic freq. estimator vs. no. of data samples.

Table Captions:

Table 1. Comparisons of truncated least-squares methods.

Figure Captions:

Fig. 1 Block diagram for sinusoidal frequency estimation based on the FBLP model.

Fig. 2 Average fractional truncated Frobenius norms.

Fig. 3 Mean frequency estimates for $f_1 = .125$ using a 24×36 FBLP matrix.

Fig. 4 Mean frequency estimates for $f_2 = .135$ using a 24×36 FBLP matrix.

Fig. 5 Standard deviations for estimating $f_1 = .125$ using a 24×36 FBLP matrix.

Fig. 6 Standard deviations for estimating $f_2 = .135$ using a 24×36 FBLP matrix.

Fig. 7 Mean distances to unit circle of the roots of the 1st harmonic freq. estimator vs. SNR.

Fig. 8 Mean distances to unit circle of the roots of the 2nd harmonic freq. estimator vs. SNR.

Fig. 9 Mean distances to unit circle of the roots of the 3rd (false) harmonic freq. estimator vs. SNR

Fig.10 Mean freq bias vs. no. of data samples for $f = \{.125, .135\}$, SNR=10dB, and order=36.

Fig.11 Standard deviations of estimates vs. no. of data samples for $f = \{.125, .135\}$, SNR=10dB, and order=36.

Fig.12 Mean distances to unit circle of the roots of the 3rd (false) harmonic freq. estimator vs. no. of data samples.